Anal Bioanal Chem (2016) 408:5829–5841
DOI 10.1007/s00216-016-9695-5

RESEARCH PAPER

Assessment of the effects of As(III) treatment on cyanobacteria lipidomic profiles by LC-MS and MCR-ALS

Aline S. Marques[1] · **Carmen Bedia**[2] · **Kássio M. G. Lima**[1] · **Romà Tauler**[2]

Received: 3 April 2016 / Revised: 25 May 2016 / Accepted: 6 June 2016 / Published online: 16 June 2016
© Springer-Verlag Berlin Heidelberg 2016

Abstract Cyanobacteria are a group of photosynthetic, nitrogen-fixing bacteria present in a wide variety of habitats such as freshwater, marine, and terrestrial ecosystems. In this work, the effects of As(III), a major toxic environmental pollutant, on the lipidomic profiles of two cyanobacteria species (*Anabaena* and *Planktothrix agardhii*) were assessed by means of a recently proposed method based on the concept of regions of interest (ROI) in liquid chromatography mass spectroscopy (LC-MS) together with multivariate curve resolution alternating least squares (MCR-ALS). Cyanobacteria were exposed to two concentrations of As(III) for a week, and lipid extracts were analyzed by ultrahigh-performance liquid chromatography/time-of-flight mass spectrometry in full scan mode. The data obtained were compressed by means of the ROI strategy, and the resulting LC-MS data sets were analyzed by the MCR-ALS method. Comparison of profile peak areas resolved by MCR-ALS in control and exposed samples allowed the discrimination of lipids whose concentrations were changed due to As(III) treatment. The tentative identification of these lipids revealed an important reduction of the levels of some galactolipids such as monogalactosyldiacylglycerol, the pigment chlorophyll a and its degradation product, pheophytin *a*, as well as carotene compounds such as 3-hydroxycarotene and carotene-3,3′-dione, all of these compounds being essential in the photosynthetic process. These results suggested that As(III) induced important changes in the composition of lipids of cyanobacteria, which were able to compromise their energy production processes.

Keywords LC-MS · MCR-ALS · Cyanobacteria · As(III)

✉ Romà Tauler
roma.tauler@idaea.csic.es

[1] Biological Chemistry and Chemometrics, Universidade Federal do Rio Grande do Norte (UFRN-IQ), Natal 59071-970, Brazil

[2] Institute of Environmental Assessment and Water Diagnostic (IDAEA-CSIC), Jordi Girona 18-26, 08028 Barcelona, Spain

Introduction

Arsenic (As) is a well-known toxic element naturally present in the Earth's crust [1]. Several studies have shown the different responses of microorganisms exposed to this metal, such as the demethylation process in fungi [2], contamination in food [3], and bioaccumulation, transformation, and release in *Microcystis* [4]. Arsenic is considered to be one of the most toxic environmental substances. Both natural and anthropogenic sources contribute to the presence of As in environmental media [5].

Cyanobacteria are the only known prokaryotes that perform oxygen-evolving photosynthesis, commonly found in diverse environments including marine and freshwater, as well as in terrestrial habitats [6]. They are responsible for about 50 % of earthly photosynthesis, and they are the main contributors of the global oxygen cycle. Metals, such as arsenic, are known to exercise a negative influence on cyanobacteria photosynthesis [7, 8]. Cyanobacteria photosynthetic processes are known to occur in cyanobacteria thylakoid membrane [9]. Lipids of cyanobacteria have an important function in the thylakoid membrane structural components, and consequently, they are vital for their life processes [10]. The lipid composition of cyanobacteria thylakoid membrane is mostly formed by galactolipid species of monogalactosyldiacylglycerol (MGDG) and digalactosyldiacylglycerol (DGDG). These lipids are crucial for the stability and activity of photosynthesis systems [11]. A decrease in their concentration has been related to a reduction

of the photosynthetic activity, changes in chloroplast ultrastructure, and growth arrest [12].

Liquid chromatography coupled to mass spectrometry (LC-MS) is currently being employed in lipid analysis due to its high resolution and sensitivity, enabling the simultaneous identification of multiple constituents in the same analyzed sample [13]. However, this analytical methodology, when applied in complex lipidomic studies, generates a huge amount of data in the analysis of a single biological sample [14]. A recently introduced strategy of selection of mass spectrometry regions of interest (ROIs) is proposed to handle the extremely large size of these LC-MS data sets, using affordable computer resources, without mass accuracy loss [15]. The ROI-based method significantly decreases the size of LC-MS data sets, allowing simultaneous analysis of multiple data sets in the study of the same system under different experimental conditions.

Multivariate curve resolution alternating least squares (MCR-ALS) is a chemometric tool applied to resolve multicomponent responses from unknown unresolved mixtures [16–19]. MCR-ALS has been applied to the resolution of elution/concentration and mass spectra profiles for the different components existing in complex cell lipid mixtures analyzed by chromatographic methods [14]. Recently, it has also been applied successfully to resolve complex omics profiling problems, such as in lipidomics [18, 19] and metabolomics [20] studies.

The aim of this work was to evaluate the changes operating on lipidomic profiles of cyanobacteria (*Anabaena* and *Planktothrix agardhii*) when they were treated with As(III). As_2O_3 was selected as a source of As(III) since it is the main precursor of most of As compounds [21]. To accomplish this objective, a recently introduced data analysis strategy which combines the ROI concept in LC-MS together with MCR-ALS was applied. Changing lipids were identified and preliminary biochemical interpretations of the results are discussed.

Materials and methods

Chemicals and solvents

As_2O_3 was purchased from Sigma. Analytical grade methanol and chloroform were purchased from Merck and Carlo Erba, respectively. HPLC Gradient Grade acetonitrile was purchased from Fischer Chemicals. Lipid standards were obtained from Avanti Polar Lipids.

Cyanobacteria culture and As(III) exposure

Anabaena and *P. agardhii* were both obtained from Culture Collection of Algae and Protozoa (CCAP1403/21 and CCAP1459/11, respectively; SAMS Limited) and were grown aseptically in 500-mL Erlenmeyer flasks containing BG-11 medium (with $NaNO_3$ as a source of nitrogen) [22] at 25 °C under continuous fluorescent white light with an intensity of 15 μmol photons m^{-2} s^{-1}, until an optical density of 0.1–0.2 at 750 nm (OD_{750}) was reached. Then, the cultures were transferred to 50-mL Falcon flasks with different concentrations (0, 1, and 2 mM) of As(III); cells were maintained in the mentioned conditions for 7 days. The choice of these As(III) concentrations is based on a previous toxicity test on cyanobacteria (data not shown) in which the concentration 1 mM started to reduce normal cell growth.

Estimation of protein content

Protein content was measured using Pierce™ BCA Protein Assay Kit (Thermo Scientific). Bovine serum albumin was used as a protein standard. In a 96-well plate, 20 μL of every sample was mixed with 100 μL of the working solution (BCA reagents A and B, 1:50) and then incubated at 37 °C for 1 h. Absorbance was measured at 562 nm (Synergy 2 Multi-Mode Reader, Biotek Instruments, Inc.).

Microscopy and chlorophyll spectra

Cyanobacteria were visualized through a Nikon eclipse 90i microscope using a ×60 oil objective, and images were captured with a Nikon DS-Ri1 digital camera. Chlorophyll spectra were measured in a Synergy 2 Multi-Mode Reader (Biotek Instruments, Inc.) UV–Visible spectrophotometer in the range of 300–800 nm.

Lipid extraction

For every sample, 250 mL of cyanobacteria cultured in 500-mL Erlenmeyer flasks was used. Cyanobacteria cultures were centrifuged (5000 rpm, 20 min, 4 °C) and the supernatants were discarded to recover cell pellets. The extraction has been performed as previously described [19]. Briefly, 100 μL of Mili-Q water was added to the cyanobacteria pellets and the suspension was transferred to borosilicate glass tubes. This was followed by the addition of 500 μL of chloroform and 250 μL of methanol in each tube. This mixture was fortified with different internal standards of lipids (C18(plasmalogen)-18:1 phosphatidylcholine, C18(plasmalogen)-18:1 phosphatidylethanolamine, C16(plasmalogen) lysophosphatidylcholine, 1,2,3-17:0 triacylglycerol, 1,3-17:0 D5 diacylglycerol, 17:0 monoacylglycerol, 17:0 cholesteryl ester, 16:0 D31-18:1 phosphatidic acid, 16:0 D31-18:1 phosphatidylcholine, 16:0 D31-18:1 phosphatidylethanolamine, 16:0 D31-18:1 phosphatidylserine, 16:0 D31-18:1 phosphatidylglycerol, 16:0 D31-18:1 phosphatidylinositol, 17:1 lysophosphatidylcholine, 17:1 lysophosphatidylglycerol, 17:1 lysophosphatidylserine, 17:1 lysophosphatidic acid, 17:1 lysophosphatidylcholine,

17:1 lysophosphatidylinositol), 200 pmol each (10 μL of 20 μM stock solutions in absolute ethanol). Next, samples were vortexed and sonicated until they appeared dispersed. In order to increase the efficiency of the extraction, samples were left under agitation overnight in a water bath at 48 °C, as described previously for other lipid extractions [23]. Samples were then cooled and evaporated under N_2 stream and subsequently re-suspended in 500 μL of methanol. The resulting suspension was then transferred to 1.5-mL Eppendorf tubes and evaporated again. Then, samples were resuspended in 150 μL of methanol and were centrifuged (10,000 rpm, 3 min) to discard all precipitates from the samples. Finally, 130 μL of each sample supernatant was taken and transferred to UPLC vials for LC injection.

Liquid chromatography mass spectrometry

LC-MS analysis was performed using a Waters Acquity UPLC system connected to a Waters LCT Premier orthogonal accelerated time-of-flight mass spectrometer (Waters) operated in positive ion electrospray ionization mode. Full scan spectra from 50 to 1800 Da were acquired, and acquisition of every MS spectrum was taken approximately 0.2 s.

Mass accuracy and reproducibility were maintained by using an independent reference spray via the LockSpray interference. The analytical column was a 100 × 2.1-mm inner diameter, 1.7-μm C8 Acquity UPLC bridged ethylene hybrid (Waters). The two mobile phases were: phase A, H_2O 2 mM ammonium formate, and phase B, MeOH 1 mM ammonium formate. Both contained 0.2 % of formic acid. The flow rate was 0.3 mL min^{-1}. Tthe gradient of A/B solvents started at 20:80 and changed to 10:90 in 3 min, from 3 to 6 min remained at 10:90, changed to 1:99 in 6 min until minute 15, remained 1:99 until minute 18, and finally returned to the initial conditions until minute 20. The column was held at 30 °C.

Chemometric data analysis

Raw data files obtained from the LC-MS analysis of every sample were transformed to CDF format by Databridge function of MassLynx™ V. 4.1 software. LC-MS data were uploaded into the MATLAB workspace environment (version R2012b, The Mathworks Inc.) using the functions mzcdfread and mzcdf2peaks of the Bioinformatics Toolbox (The Mathworks Inc.). LC-MS data were arranged and aligned according to their *m*/*z* values in a square regular data matrix, with retention times in the rows and selected *m*/*z* values in the columns. Different strategies were adapted to build such a data matrix. We have recently proposed a new protocol based on the selection of the ROIs [15]. This strategy allows for the selection of *m*/*z* traces whose intensity signals are higher than preselected threshold values (not noise or spurious measurements), and it takes advantage of the sparsity of the measured MS data and of their mass accuracy. Using this approach, full-scan chromatographic MS matrices with the highest experimental mass accuracy are obtained with low storage requirements. A relatively low number (200–500) of high-resolution MS (intensity, *m*/*z*) signals were finally taken into account, with more than 100-fold computer storage reduction (Fig. 1).

Every MS-ROI data matrix was then normalized taking into account the areas of the internal standards added and the protein content measured for each sample. This normalization was done by multiplying each matrix by a factor obtained as follows: (200 × mg protein)/mean area of standards, where 200 refers to the picomoles of standards added in the lipid extraction. After normalization, individual MS-ROI matrices obtained in the analysis of every *Anabaena* and *P. agardhii* samples were used to build four different augmented matrices. In Fig. 1, the exemplary construction of a MS-ROI augmented matrix was given. Since MS-ROI individual data matrices have different number of ROI *m*/*z* values, a preliminary step of ROI rearrangement to consider all those ROI *m*/*z* values (common and not common) with significant traces (retention times where MS intensity values are higher than the threshold values at the considered ROI *m*/*z* value) is performed. In case an individual matrix does not have a particular significant trace at this ROI *m*/*z* value, low random intensity values at the noise level are assigned. See Gorrochategui et al. [15] for more details about MS-ROI augmented matrix building. As shown in Fig. 1, the MS-ROI augmented data matrix $\mathbf{D}_{aug}$ is built with four control samples and four treated samples, and the final dimensions of this augmented matrix are the total number of retention times considered in the eight chromatographic runs times the number of finally considered *m*/*z* ROI values. The first MS-ROI augmented matrix was built with the four non-treated (control) and the four 1-mM As(III)-treated *Anabaena* samples. The second MS-ROI augmented matrix had the four non-treated (control) and the four 2-mM As(III)-treated *Anabaena* samples. The third MS-ROI augmented matrix had the four non-treated (control) and the four 1-mM As(III)-treated *P. agardhii* samples. Finally, the fourth MS-ROI augmented matrix was built with the four non-treated (control) and the four 2-mM As(III)-treated *P. agardhii* samples. In order to perform this matrix augmentation column-wise, the columns of every ROI data matrix should have the same *m*/*z* ROI values. See Gorrochategui et al. [15] for details on how to implement this in practice.

In this work, the MCR-ALS method [16, 17] has been used for the analysis of the augmented ROI data matrices described above. Since the MCR-ALS method has been described

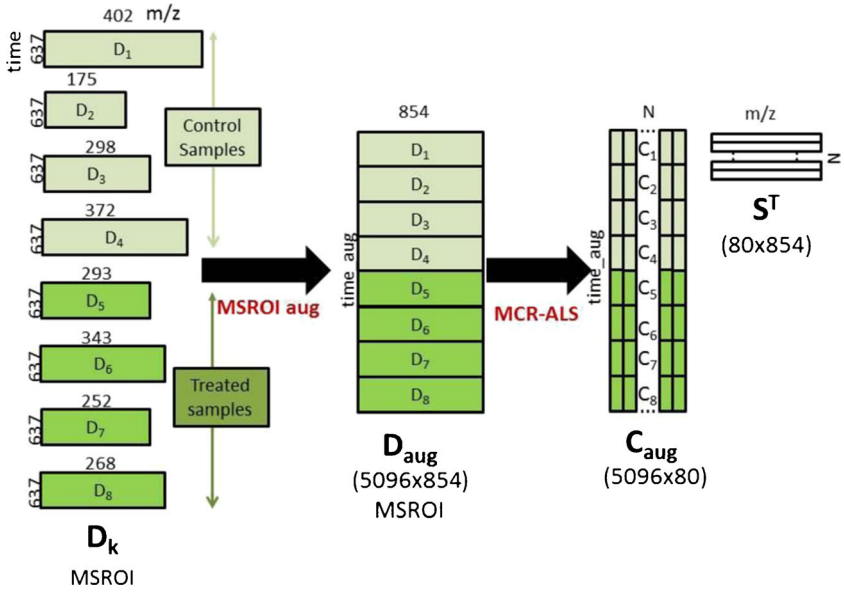

Fig. 1 Example of MS-ROI data matrix augmentation and application of MCR-ALS to the simultaneous analysis of eight individual MS-ROI data matrices: four control samples and four treated samples. See [15] and Eq. 2

elsewhere [15–17], only a brief explanation is given below. This method is based on the fulfillment of a bilinear measurement model, which assumes that the measured MS spectra along the chromatographic separation are the sum of the MS spectra of the lipids of the investigated system (plus some background, solvent, and instrumental noise contributions) weighted by their relative concentrations. This bilinear model can be described by the simple data matrix equation

$$\mathbf{D} = \mathbf{C}\mathbf{S}^{\mathbf{T}} + \mathbf{E} \quad (1)$$

In the case of a single LC-MS-ROI data matrix, **D** contains the MS intensity signals at the selected *m*/*z* ROI values (columns) and retention times (rows). **C** has the elution or concentration profiles of resolved components, and $\mathbf{S}^{\mathbf{T}}$ has the resolved pure MS-ROI spectra of these components. **E** has the non-explained variance and experimental error. MCR-ALS solves Eq. 1 by an Alternating Least Squares algorithm which calculates iteratively the concentration, **C**, and the pure MS-ROI spectra, $\mathbf{S}^{\mathbf{T}}$, matrices fitting optimally the experimental data matrix, **D**. MCR-ALS optimization requires the initial proposal of a number of components and of an initial estimate of either the **C** or $\mathbf{S}^{\mathbf{T}}$ matrix. A sufficiently large number of components (for instance, 80 or more) can be initially selected to explain most of the data variance (e.g., more than 90 % of the total data variance) and to properly describe the experimental data features (chromatographic peaks). This number of components can also include some components that are not strictly related to the lipid signals but to the solvent, background, or other detector and instrumental signal contributions. Initial estimates of either the **C** or $\mathbf{S}^{\mathbf{T}}$ matrix are obtained from the more distinct rows (MS spectra) or columns (chromatograms) of the data matrix. These are good initial estimates for MCR-ALS due to the high selectivity of the LC-MS data. Once the number of components and initial estimates of either **C** or $\mathbf{S}^{\mathbf{T}}$ are provided, during the ALS optimization, various constraints are applied to model appropriately the shapes of the **C** and $\mathbf{S}^{\mathbf{T}}$ profiles [24]. For ROI LC-MS data, non-negativity was applied to ensure the concentration and spectral profiles to be positive. Also, during the ALS optimization, the MS spectra were normalized to have all maximum intensity equal to 1, to avoid scale indeterminacies (intensity ambiguity) and to give relative quantitative information in the concentration profiles. Since the MS-ROI spectra are sparse and very selective (a lot of zero values), rotation ambiguities [25] are practically not present in this case. Fitting MCR-ALS results can be performed by using the explained data variance calculated as: $R^2(\%) = \sum d_{ij}^2 / \sum d_{ij}^2 \times 100$, where $i = 1,\ldots,I$ (number of data matrix rows, retention values) and $j = 1,\ldots,J$ (number of data matrix columns, number of *m*/*z* ROI values), d_{ij} is the MS-ROI individual intensity value in the experimental matrix **D**, and d^*_{ij} is the corresponding value calculated by MCR-ALS using the optimal **C** and $\mathbf{S}^{\mathbf{T}}$ matrices finally obtained, as has been shown in previous works [16, 17].

The MCR-ALS bilinear model can be extended to the simultaneous analysis of multiple individual data matrices using the column-wise augmentation strategy described in Fig. 1. In this particular case, the simultaneous analysis of multiple MS-ROI data matrices coming from the same type of cyanobacteria culture (either *Anabaena* or *P. agardhii*) under different conditions (control samples and As(III)-treated samples at two concentrations, 1 and 2 mM) was performed using the appropriate MS-ROI column-wise augmented data matrix (see Fig. 1). Equation 1 for MCR analysis of a single data matrix is now extended

to Eq. 2 for MCR analysis of the new column-wise MS-ROI augmented data matrices [16, 17].

$$\begin{pmatrix} \mathbf{D}_1 \\ \mathbf{D}_2 \\ \mathbf{D}_3 \\ \dots \\ \mathbf{D}_K \end{pmatrix} = \begin{pmatrix} \mathbf{C}_1 \\ \mathbf{C}_2 \\ \mathbf{C}_3 \\ \dots \\ \mathbf{C}_k \end{pmatrix} \mathbf{S}^T + \begin{pmatrix} \mathbf{E}_1 \\ \mathbf{E}_2 \\ \mathbf{E}_3 \\ \dots \\ \mathbf{E}_k \end{pmatrix} = \mathbf{C}_{aug}\mathbf{S}^T + \mathbf{E}_{aug} \quad (2)$$

In this equation, the column-wise augmented MS-ROI data matrix, $\mathbf{D}_{aug}$, is decomposed by the bilinear model into the product of a column-wise augmented matrix, $\mathbf{C}_{aug}$, having the elution profiles of the resolved components in every individual MS-ROI data matrix, by the MS spectra matrix, $\mathbf{S}^T$, having the pure MS-ROI spectra of these components. $\mathbf{E}_{aug}$ is the corresponding matrix which will have the model unexplained variance (for the considered number of components) and experimental error. It is important to remark here that the proposed MCR-ALS data analysis strategy does not imply any shift nor shape assumption nor correction of the chromatographic elution profiles of the same component in the different chromatographic runs. It only needs that the *m*/*z* values match among the different MS spectra included in **D** or $\mathbf{D}_{aug}$ and that every component can be defined by a unique pure MS spectrum. This data analysis procedure has high flexibility and resolution power, it takes profit of the high resolution of the MS detector, and it allows for the lack of reproducibility of chromatographic separation conditions.

Once the MCR-ALS results are obtained, the $\mathbf{C}_{aug}$ and $\mathbf{S}^T$ matrices are examined in detail to extract qualitative (identification) and quantitative information and to allow the interpretation of the investigated effects (by As(III) treatment). The elution/concentration profiles resolved by MCR-ALS for every component are in the columns of the $\mathbf{C}_{aug}$ matrix for all chromatographic runs simultaneously analyzed. Comparison of the areas of these elution profiles provides the relative quantitative information about a particular resolved component in the different analyzed samples. Comparison of the areas between the control and As(III)-treated samples allows for the statistical assessment of the produced effects at a particular significance level (*p* values below 0.05). Only those components showing statistically significant differences between their concentrations (peak areas) in the control and As(III)-treated samples are further considered for their chemical compound identification. This identification is performed looking for the MCR-ALS MS-ROI-resolved spectrum corresponding to the same component in the $\mathbf{S}^T$ matrix. The *m*/*z* ROI values of these spectra have full-scan MS mass accuracy and are used for compound identification using the Human Metabolome Database (http://www.hmdb.ca) and Lipid Maps (http://www.lipidmaps.org) online databases. Lipids are assigned from *m*/*z* values associated to smaller delta values (difference between query mass and adduct mass), and they were compared with those found in previous works.

Results

Morphological changes and chlorophyll content of cyanobacteria exposed to arsenic

First, morphological changes of cyanobacteria (*Anabaena* and *P. agardhii*) were assessed after 7 days of arsenic exposure. As depicted in the optical microscope images of Fig. 2, cyanobacteria filaments showed a visible decrease of green coloration along with the increasing concentration of As(III). At 2 mM As(III), *P. agardhii* species presented considerable fading of their green pigmentation while *Anabaena* species showed complete discoloration.

Since green pigmentation in cyanobacteria is associated with the composition of photosynthetic pigments like chlorophyll [6], changes in this green pigmentation were first analyzed by UV–Visible spectrometry (Fig. 3).

The absorbance spectra of treated cyanobacteria were recorded. The results showed that absorption bands between 400 and 500 nm were practically eliminated after arsenic treatment, especially in the case of *Anabaena* (Fig. 3A). Considering that the main peak of chlorophyll is around 450 nm [26], the results suggested that the decrease of green coloration was related to chlorophyll degradation. An important decline of chlorophyll under arsenic exposure has already been described in previous works [4]. Rocchetta et al. [27] also showed that algal cells exposed to heavy metals such as copper and chromium suffered from multiple biochemical alterations affecting the photosynthesis. In this work, in order to study the changes in lipid composition due to As(III) treatment, an exhaustive untargeted lipidomic study was performed.

Chemometric analysis of LC-MS data of cyanobacteria exposed to As(III)

The effects of different concentrations (0, 1, and 2 mM) of arsenic after 7 days of exposure on the two cyanobacteria (*Anabaena* and *P. agardhii*) cultures were investigated by LC-MS in positive ion mode. LC-MS raw data were first normalized (using internal standards and total protein content) and compressed according to the ROI strategy (see "Materials and methods"). As mentioned, the use of the ROI strategy allowed substantial reduction of computer storage and processing time without losing mass accuracy [15].

In Fig. 4, the positive ion mode full-scan LC-MS chromatograms (after selection of the ROIs) are compared for

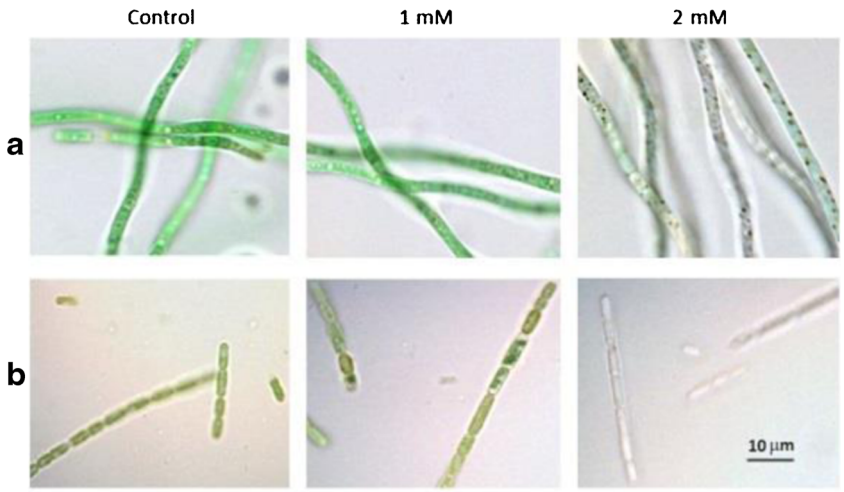

Fig. 2 Light microscope pictures of cyanobacteria filaments under As(III) treatment. *Anabaena* (**a**) and *P. agardhii* (**b**) cyanobacteria species incubated for 7 days with 0, 1, and 2 mM of As(III) in Blue-Green medium

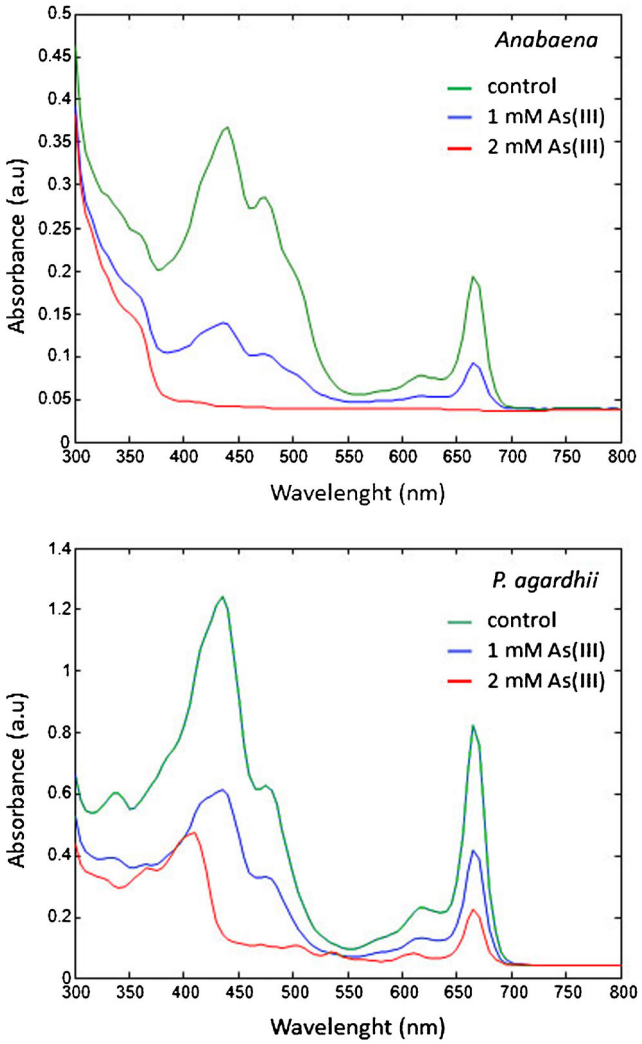

Fig. 3 Chlorophyll absorption spectra of As(III)-treated cyanobacteria. *Anabaena* (**a**) and *P. agardhii* (**b**) exposed for 7 days to 0, 1, and 2 mM As(III) (*brown*, *blue*, and *yellow lines*, respectively)

samples extracted from *Anabaena* cultures without any As(III) treatment (Fig. 4A) to those obtained after 7 days of exposure with 1 mM As(III) (Fig. 4B). Distinct features are clearly noticed in these chromatograms already showing the effects of metal treatment.

In order to investigate the effects on lipid concentration changes in both cyanobacteria cultures due to the As(III) treatment at 1 and 2 mM, four different MS-ROI column-wise augmented data matrices were built. Each new column-wise augmented data matrix contained eight MS-ROI individual data matrices, the first four being the control replicates and the last four the treatment replicates, as explained in "Materials and methods." In Fig. 5, the first MS-ROI augmented matrix for *Anabaena* at 1-mM As(III) treatment is shown as an example.

The eight chromatographic sections distinguished correspond to the eight investigated samples. As shown in the picture, plots of the LC-MS-ROI data for the control samples (four regions on the left) had higher intensity signals than the plots of the four 1-mM As(III)-treated samples (four regions on the right), suggesting an important loss of lipid species concentrations due to the As(III) treatment.

The augmented LC-MS-ROI data matrices of four control and four treated cyanobacteria samples were then analyzed by MCR-ALS (see Fig. 1), using non-negativity constraints, to resolve elution and spectral profiles of the sample lipid constituents. MS-resolved pure spectra ($\mathbf{S}^{\mathbf{T}}$) were also normalized to have the same equal intensity, transferring all relative quantitative information to elution profiles (**C**). MCR-ALS was performed using a large enough number of components (80) to explain enough data variance and to assure the resolution of a sufficiently large number of elution and MS spectra profiles with reasonable chemical shapes. In the four cases, *f*, the explained variances were between 93 and 95 %. A small number of the MCR-ALS-resolved components could be related to solvent and background contributions, whereas all other had

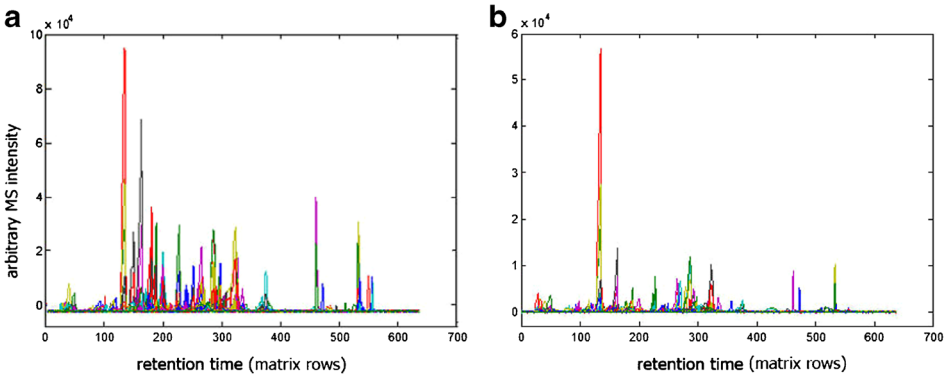

Fig. 4 LC-MS-ROI chromatogram of a single sample (from one single-data matrix). *Anabaena* control (**a**) and 1-mM As(III)-treated (**b**) samples. In the *X*-axis are the number of retention times in the analysis of one sample (giving one data matrix with 637 rows or retention times; see Fig. 1)

reasonable chromatographic and spectral shapes and features. Only these ones were investigated in more detail, and their concentration changes between the control and As(III)-treated samples were estimated.

Once the elution profiles corresponding to the same component in the control and treated samples of the same augmented MS-ROI matrix were resolved, they were further analyzed to assess the possible concentration changes due to As(III) treatment. As explained in "Materials and methods," this was performed by comparison of the peak areas and/or heights of these two types of samples. A statistical Student's *t* test was used in every case to assess for the statistical difference between the peak areas/heights of the elution profiles of the same component in the control and treated samples. As an example, the MCR-ALS-resolved elution profiles and mass spectra for two components that presented significant changes between controls and treatments are represented in Fig. 6 for both *Anabaena* 1-mM and *P. agardhii* 1-mM augmented matrices. On one hand, in *Anabaena* 1-mM samples on the left of Fig. 6, component 79 exhibited an important decrease in the treated samples (four sections on the right), as shown in Fig. 6A, with an *m*/*z* ROI value of 800.6217 (Fig. 6B), which was further identified as MGDG(36:2). In the case of *P. agardhii* 1-mM samples on the right of Fig. 6, component 21 presented a similar decreasing profile in the treated samples (Fig. 6E). With an *m*/*z* ROI value of 551.4229 (Fig. 6F), this molecule was further identified as 3-*cis*-hydroxy-carotene. Bar plots of the areas and the heights of the resolved peaks in both examples represented in both cases (Fig. 6C, D, G, H) also confirmed the changes produced by As(III) treatment.

In Tables 1 and 2, lipids showing significant changes according to the *t* test (at the $p < 0.05$ significance level) are

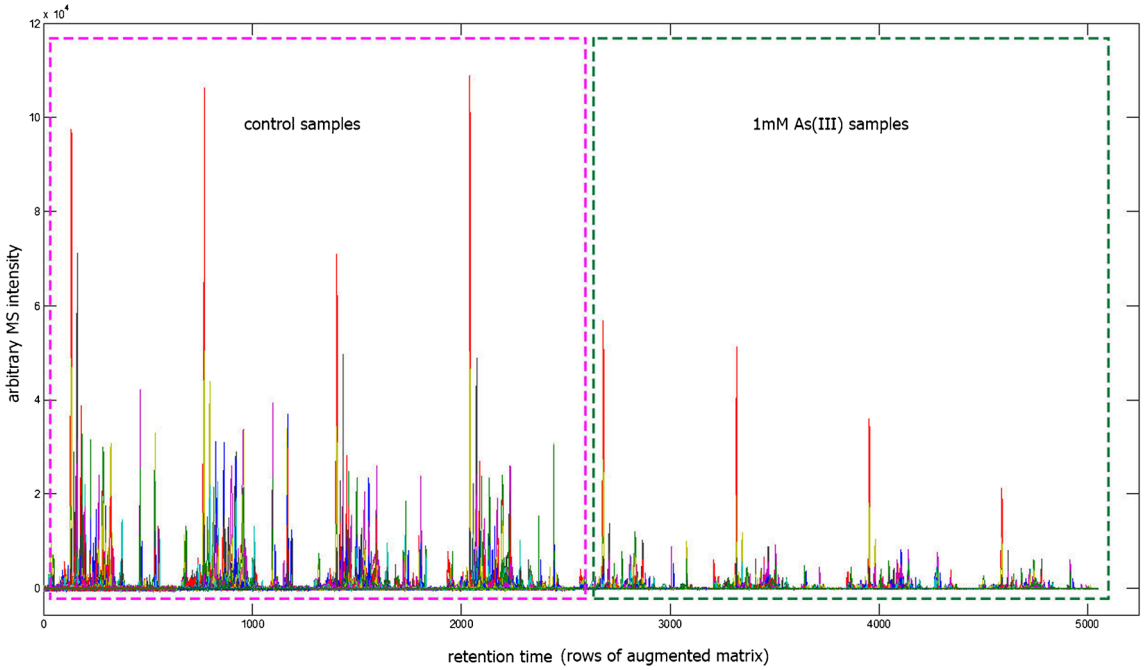

Fig. 5 LC-MS-ROI chromatograms of multiple samples (from one column-wise augmented data matrix). On the *left* are four *Anabaena* control samples (section marked on *pink slashed square*). On the *right* are four 1-mM As(III)-treated samples (section marked on *green slashed square*). In the *X*-axis are the total number of retention times in the analysis of the eight samples (giving one column-wise augmented data matrix with $8 \times 637 = 5096$ rows or retention times; see Fig. 1)

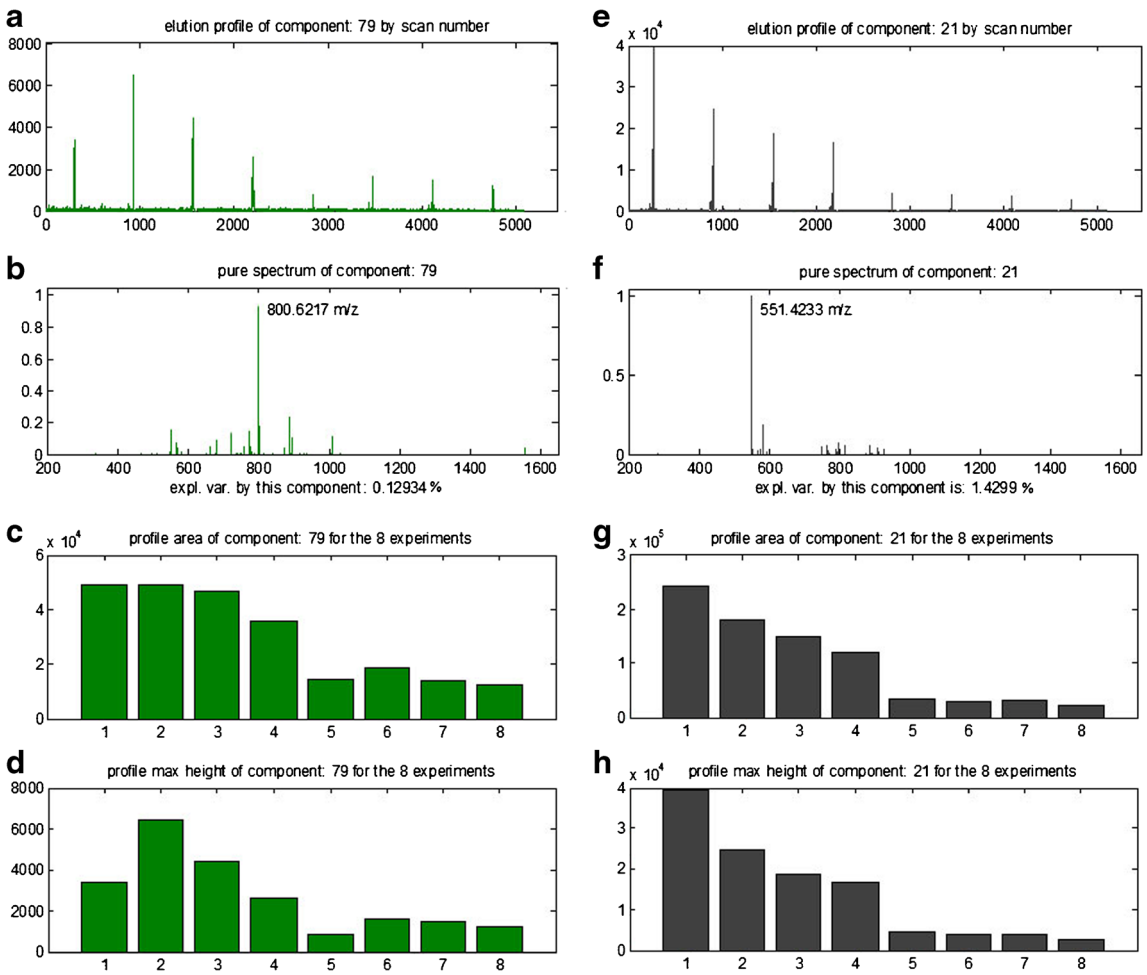

Fig. 6 Examples of results obtained in the MCR-ALS simultaneous analysis of multiple LC-MS-ROI chromatograms (from the MCR-ALS analysis of column-wise augmented data matrices having four control samples and four 1-mM As(III)-treated samples; see Eq. 2). Results are given for component 79 (*left*) in the analysis of *Anabaena* sample and for component 21 (*right*) in the analysis of *P. agardhii* sample. **a**, **c** MCR-ALS-resolved elution profiles ($\mathbf{C}_{aug}$ in Eq. 2). **b**, **f** MCR-ALS-resolved MS pure spectra ($\mathbf{S}^{T}$ in Eq. 2) with the *m*/*z* ROI values at their intensity maxima. **c**, **g** Bar plots of the integrated peaks areas of each replicate. **d**, **h** Bar plots of the peaks heights of each replicate

listed with their retention times, measured *m*/*z*, explained variance (R^2), identified compounds, adduct, calculated *m*/*z*, mass error (in parts per million), area and height fold changes, and *p* values. These lipids are given and summarized for *Anabaena* and *P. agardhii* cyanobacteria cultures treated with 1 and 2 mM As(III), respectively. Most of the listed lipids are associated with cyanobacteria membranes and with pigments related to the photosynthesis process. Interestingly, at 1-mM As(III) treatment (Table 1), a 4- to 5-fold decrease of several MGDG species has been detected for both cyanobacteria species. These galactolipids are associated with cyanobacteria membrane and are known to be involved in thylakoid membrane packing and to provide a mechanism for the separation of the components of the photosystem within the thylakoid membrane [12]. In addition, as mentioned before, we observed a significant loss in the concentrations of pigments related to the photosynthetic system in 1-mM *Anabaena* samples, such as chlorophyll a, and its sub-product, pheophytin a. Also, we found a large 4-fold decrease of some carotene compounds such as 3-*cis*-hydroxy-carotene and carotene-3,3′-dione. Carotenes have key roles in light absorption for use in the photosynthesis process, as well as a protective role of chlorophyll from photodamage [28]. In *P. agardhii*, we also found a significant 5-fold decrease of 3-*cis*-hydroxy-carotene, as has been shown in the example of Fig. 6. Another interesting feature observed is the decrease of triacylglycerol (51:0), only found in *Anabaena* samples.

Similar results were obtained for 2-mM As(III) treatment (Table 2). In this case, the decrease of MGDGs that showed a reduction in their levels at 1 mM was more intense in both cyanobacteria. Also, a new MGDG appeared reduced at this concentration. In *Anabaena* samples, the decline of pheophytin and carotene concentrations was more pronounced (more than 10-fold). For *P. agardhii* samples, pheophytin a appeared reduced in the treated samples, and the reduction of 3-*cis*-hydroxy-carotene levels observed at

Table 1 Summary of molecules that showed significant changes between untreated and 1-mM As(III)-treated samples for both *Anabaena* and *P. agardhii* using the proposed LC-MS-ROI-MCR-ALS methodology

RT	Measured *m/z*	R^2	Identified compound	Adduct	calculated *m/z*	Mass error (ppm)	Area fold change	Height fold change	Area *p* value	Height *p* value
Anabaena 1 mM										
9.12	551.4229	3.0424	3-*cis*-Hydroxy-b.e-carotene *b	M+H	551.4253	4.4	0.21	0.25	0.002	0.001
5.17	565.4057	0.1326	E.e-carotene-3.3′-dione *b	M+H	565.4040	3.0	0.28	0.15	0.041	0.029
12.93	567.4538	0.7971	Unknown	–	–	–	0.18	0.16	0.003	0.002
3.49	583.4128	0.1129	Diatoxanthin 3.6-epoxide *b	M+H	583.4146	3.0	0.21	0.15	0.001	0.007
11.55	619.6013	0.1602	Unknown	–	–	–	0.38	0.34	0.001	0.001
1.32	626.1850	0.2677	Unknown	–	–	–	0.19	0.15	0.015	0.035
4.58	675.6788	35.879	Unknown	–	–	–	0.40	0.43	0.026	0.019
16.29	686.6451	0.1356	Unknown	–			0.39	0.42	0.004	0.001
6.16	766.5462	0.815	MGDG(34:5) *a	$[M+NH_4]$	766.546	0.3	0.18	0.11	0.016	0.022
10.21	800.6217	0.1293	MGDG(36:2) *a	$[M+NH_4]$	800.6247	3.7	0.33	0.30	0.001	0.027
18.4	866.8210	1.1585	TG(51:0)	$[M+NH_4]$	866.818	3.5	0.11	0.09	0.017	0.032
11.11	871.5736	4.8752	Pheophytin a*b	[M+Na]	871.5737	0.2	0.14	0.21	0.039	0.001
9.84	893.5477	2.2746	Chlorophyll a*b	[M+H]	893.542589	5.7	0.21	0.12	0.018	0.007
P. agardhii 1 mM										
3.96	310.3083	0.0651	Unknown	–	–	–	0.3	0.4	0.0093	0.0116
9.15	551.4233	1.4298	3-*cis*-Hydroxy-b.e-carotene *b	M+H	551.4253	3.6	0.2	0.2	0.0101	0.0224
12.91	567.4542	0.5982	Unknown	–	–	–	0.2	0.2	0.0556	0.0086
1.66	594.1597	0.165	Unknown	–	–	–	0.2	0.3	0.0336	0.0067
11.55	619.6026	0.1348	Unknown	-	-	-	0.3	0.2	0.0078	0.0065
8.06	763.5351	0.3065	MGDG(35:5) *a	[M+H]	763.536	1.2	0.2	0.2	0.0172	0.0026
6.88	768.566	9.202	MGDG(34:4) *a	$[M+NH_4]$	768.5627	4.3	0.2	0.2	0.0071	0.0071
7.22	794.5805	0.24	MGDG(36:5) *a	$[M+NH_4]$	794.5776	3.6	0.3	0.1	0.0308	0.0115

Molecules are ordered by their *m/z* values. Lipids related to cyanobacteria membranes and pigments related to the photosynthesis process have been marked with *a or *b, respectively. Fold change values >1 mean that the concentrations of the compound increased after As(III) treatment. Fold change values between 0 and 1 mean a decrease of compound concentration

Table 2 Summary of molecules that showed significant changes between untreated and 2-mM As(III)-treated samples for both *Anabaena* and *P. agardhii* using the proposed UPLC-MS-ROI-MCR-ALS methodology

RT	Measured *m/z*	R^2	Identified compound	Adduct	Calculated *m/z*	Mass error (ppm)	Area fold change	Height fold change	Area *p* value	Height *p* value
Anabaena 2 mM										
9.21	550.4159	0.4266	Unknown	–	–	–	0.03	0.010	0.013	0.034
9.12	551.4229	3.0891	3-*cis*-Hydroxy-b.e-carotene *b	M+H	551.4253	4.4	0.02	0.007	0.002	0.001
5.17	565.4064	0.1376	E.e-carotene-3.3′-dione *b	M+H	565.404007	4.2	0.09	0.039	0.038	0.027
12.93	567.4544	0.7739	Unknown	–	–	–	0.01	0.001	0.003	0.002
1.6	594.1601	0.372	Unknown	–	–	–	0.22	0.220	0.001	0.005
11.55	619.6033	0.1602	Unknown	–	–	–	0.26	0.168	0.001	0.001
1.38	626.1857	0.2845	Unknown	–	–	–	0.21	0.251	0.035	0.024
4.58	675.6788	35.492	Unknown	–	–	–	0.27	0.261	0.017	0.008
16.29	686.6452	0.1242	Unknown	–	–	–	0.10	0.049	0.007	0.003
6.16	766.5473	0.8663	MGDG(34:5)*a	$[M+NH_4]$	766.5463	0.1	0.01	0.001	0.007	0.001
8.68	772.5933	0.5143	MGDG(34:2)*a	$[M+NH_4]$	772.5933	0.0	0.02	0.003	0.010	0.041
10.21	800.6139	0.1552	MGDG(36:2)*a	$[M+NH_4]$	800.6247	13.5	0.13	0.082	0.001	0.014
11.11	871.5744	4.5519	Pheophytin a*b	[M+H]	871.5737	−0.8	0.01	0.001	0.033	0.001
P. agardhii 2 mM										
3.96	310.3089	0.0631	Unknown	–	–	–	0.10	0.14	0.0098	0.0097
1.07	495.1252	0.089	Unknown	–	–	–	0.25	0.26	0.0246	0.04
12.95	536.4350	0.3259	Unknown	–	–	–	0.03	0.03	0.0105	0.0126
9.13	551.4242	3.0649	3-*cis*-Hydroxy-b.e-carotene *b	M+H	551.4253	2.0	0.03	0.01	0.0032	0.0087
12.92	567.4532	0.573	Unknown	–	–	–	0.01	0.00	0.0366	0.0076
1.66	594.1595	0.172	Unknown	–	–	–	0.17	0.17	0.0247	0.013
11.55	619.6035	0.1387	Unknown	–	–	–	0.13	0.14	0.0064	0.0057
10.09	680.4791	0.2172	Unknown	–	–	–	0.08	0.04	0.0488	0.0457
8.07	763.5356	0.3116	MGDG(35:5)*a	[M+H]	763.5360	0.6	0.19	0.16	0.031	0.0132
6.89	768.5644	9.7156	MGDG(34:4)*a	$[M+NH_4]$	768.562	3.1	0.04	0.07	0.0033	0.0044
7.75	770.5815	6.4446	MGDG(34:3)*a	$[M+NH_4]$	770.5776	5.1	0.11	0.12	0.0601	0.0471
6.48	792.5657	4.4156	MGDG(36:6)*a	$[M+NH_4]$	792.5620	4.6	0.09	0.09	0.0656	0.0476
7.23	794.5806	0.2492	MGDG(36:5)*a	$[M+NH_4]$	794.5785	2.5	0.07	0.06	0.032	0.0182
11.15	871.5709	8.1386	Pheophytin a*b	[M+Na]	871.5737	3.3	0.06	0.06	0.0427	0.0383

Molecules are ordered by their *m/z* values. Lipids related to cyanobacteria membranes and with pigments related to the photosynthesis process have been marked with *a or *b, respectively. Fold change values >1 mean that the concentrations of the compound increased after As(III) treatment. Fold change values between 0 and 1 mean a decrease of compound concentration

1 mM was more severe (30-fold). The area fold changes of the more significant features at 1- and 2-mM As(III) treatments for both cyanobacteria species are compared and summarized in Fig. 7.

Discussion

A LC-MS-ROI-MCR-ALS methodology has been proposed to perform the untargeted lipidomic analysis of two cyanobacteria species (*Anabaena* and *P. agardhii*) after 7 days of As(III) exposure at 1 and 2 mM. The application of the ROI strategy allowed the compression of the large amount of data from full-scan LC-MS data without any loss of information. Comparison of the elution profiles resolved by MCR-ALS provided information about which lipids more significantly changed their concentration after cyanobacteria exposure to different doses of As(III). The results of these analyses revealed strong affectations on the concentrations of some chemical constituents involved in photosynthesis, which is the essential survival process of cyanobacteria. Although the changes were not identical for both species of cyanobacteria, the families of compounds affected were similar and followed the same concentration reduction pattern. Among the compounds involved in As(II) toxicity, the most significant changes were on the concentration levels of some MGDG galactolipid species. These compounds are the most abundant lipids in all photosynthetic tissues, including those of higher plants, algae, and cyanobacteria. They are directly linked to cyanobacteria membrane, with two main functions: to allow efficient packing of the thylakoid membrane and to separate the components of the photosystem within the thylakoid membrane [10]. In a previous study, it has been shown that a low ratio of MGDG to DGDG is crucial to maintain the stability and proper behavior of protein membranes [11]. In addition to galactolipids, a significant drop in the concentration of photosynthetic pigments was observed. On one hand, in *Anabaena*, chlorophyll was almost completely suppressed, as well as its sub-product, pheophytin a. The concentration loss of pheophytin a was also observed in the case of *P. agardhii* at 2 mM of As(III) treatment. On the other hand, the concentrations of some carotene compounds such as 3-*cis*-hydroxy-carotene and carotene-3,3′-dione were importantly reduced. Whereas chlorophyll a has a key role in absorbing energy from light and acting as a primary electron donor in the electron transport chain of photosynthesis, carotenes behave as allied compounds to chlorophyll in the photosynthetic process as they are able to absorb light energy and transfer it to chlorophylls and also to protect chlorophyll from photodamage. This loss of pigmentation is in agreement with the observed discoloration of cyanobacteria and with the alterations of the UV spectra of the chlorophyll of both species (the results suggest that chlorophyll a is degraded to pheophytin a, which in turn is also reduced). The strong reduction of pigment concentration levels together with the reduction of galactolipid concentration levels indicated that As(III) exposure induced a collapse of the photosynthetic process.

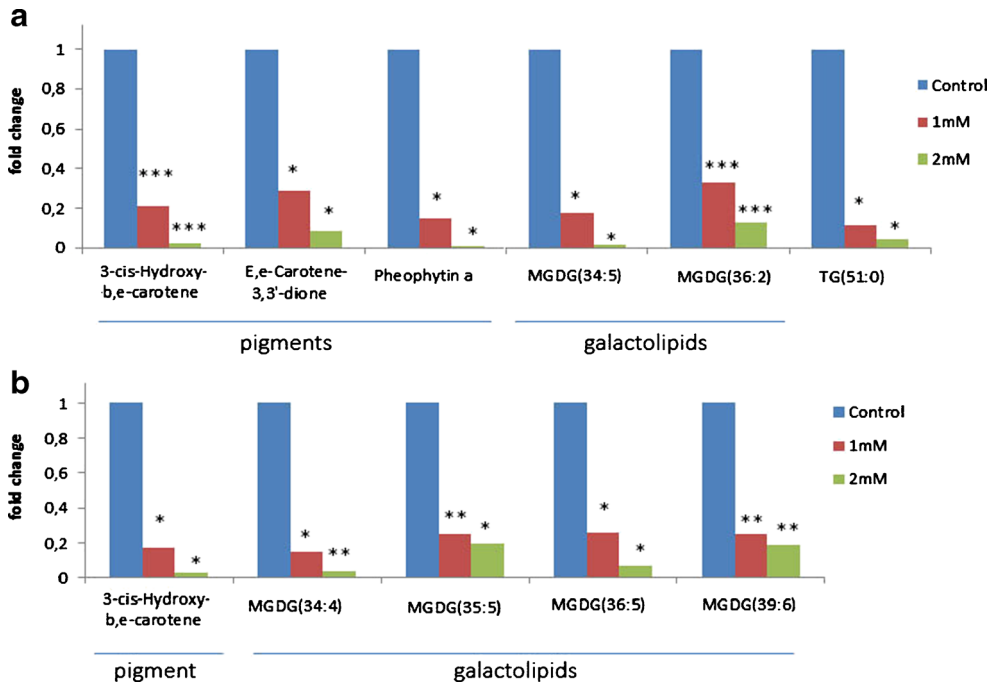

Fig. 7 Areas fold change representation of the common changing lipids observed at 1 and 2 mM of As(III) treatment for the two cyanobacteria species. Common changes between the two As(III) concentrations for *Anabaena* (**a**) and P. *agardhii* (**b**). The statistical significance of each bar is represented with *asterisks*: $*p < 0.05$, $**p < 0.01$, $***p < 0.005$

Altogether, a general disruption of the photosynthetic process has been detected after As(III) treatment in both cyanobacteria species, which reveals the strong toxicity induced by this metal, present in a variety of contamination sources.

Conclusions

The combination of a non-target methodology based on the use of the regions of interest (ROI) and multivariate curve resolution analysis on LC-MS full-scan data has been shown to be a powerful approach for the investigation of major lipidomic changes in cyanobacteria cultures when exposed to the highly toxic metal As(III). Lipid composition changes on *Anabaena* and *P. agardhii* cyanobacteria cultures when exposed for 7 days to As(III) showed that these changes were mainly associated with changes in the thylakoid cyanobacteria membrane composition (MGDG) and with photosynthetic compounds such as chlorophyll a and some carotenoids. Overall, the results of this study suggested that the presence of increasing concentrations of As(III) induced the collapse of the whole cyanobacteria photosynthetic process.

Acknowledgments The authors would like to acknowledge the financial support from the Brazilian Federal Agency for the Support and Evaluation of Graduate Education (CAPES) and Brazilian National Council for Scientific and Technological Development (CNPq) for a 1-year fellowship to Aline Marques in the Chemometrics Research Group at IDAEA-CSIC, Barcelona, Spain. K.M.G. Lima acknowledges the CNPq Grant (305962/2014-0) for financial support. This work was funded by grants from CNPq/Capes project (grant 070/2012) and by the CHEMAGEB project (FP/2007-2013)/ERC Grant Agreement no. 320737). The authors also thank Dr. Benjamín Piña and Claudia Rivetti (IDEAE/CSIC) for providing the cyanobacteria species control.

Compliance with ethical standards All authors have accepted the content of this paper and the principles of ethical and professional conduct. Sources of funding are given in the Acknowledgements section. This research has no conflict of interest and has not involved humans or animals

References

1. Ferrari SG, Silva PG, González DM, Navoni JA, Silva HJ. Arsenic tolerance of cyanobacterial strains with potential use in biotechnology. Rev Argent Microbiol. 2013;45(03):174–9.
2. Su S, Zeng X, Feng Q, Bai L, Zhang L, Jiang S, et al. Demethylation of arsenic limits its volatilization in fungi. Environ Pollut. 2015;204:141–4.
3. Phan K, Sthiannopkao S, Heng S, Phan S, Huoy L, Wong MH, et al. Arsenic contamination in the food chain and its risk assessment of populations residing in the Mekong River basin of Cambodia. J Hazard Mater. 2013;262:1064–71.
4. Wang Z, Luo Z, Yan C. Accumulation, transformation, and release of inorganic arsenic by the freshwater cyanobacterium *Microcystis aeruginosa*. Environ Sci Pollut Res. 2013;20(10):7286–95.
5. Joseph T, Dubey B, McBean EA. A critical review of arsenic exposures for Bangladeshi adults. Sci Total Environ. 2015;527–528:540–51.
6. de Oliveira VE, Neves Miranda MAC, Soares MCS, Edwards HGM, de Oliveira LFC. Study of carotenoids in cyanobacteria by Raman spectroscopy. Spectrochim Acta A Mol Biomol Spectrosc. 2015;150:373–80.
7. Yin X-X, Chen J, Qin J, Sun G-X, Rosen BP, Zhu Y-G. Biotransformation and volatilization of arsenic by three photosynthetic cyanobacteria. Plant Physiol. 2011;156(3):1631–8.
8. Cassier-Chauvat C, Chauvat F. Responses to oxidative and heavy metal stresses in cyanobacteria: recent advances. Int J Mol Sci. 2015;16(1):871.
9. Vermaas WFJ. Photosynthesis and respiration in cyanobacteria. In: Encyclopedia of life sciences. New York: Wiley; 2001. doi:10.1038/npg.els.0001670.
10. Chen D, Yan X, Xu J, Su X, Li L. Lipidomic profiling and discovery of lipid biomarkers in *Stephanodiscus* sp. under cold stress. Metabolomics. 2013;9(5):949–59.
11. Hölzl G, Dörmann P. Structure and function of glycoglycerolipids in plants and bacteria. Prog Lipid Res. 2007;46(5):225–43.
12. Dörmann P, Benning C. Galactolipids rule in seed plants. Trends Plant Sci. 2002;7(3):112–8.
13. Li S, Xu J, Jiang Y, Zhou C, Yu X, Zhong Y, et al. Lipidomic analysis can distinguish between two morphologically similar strains of *Nannochloropsis oceanica*. J Phycol. 2015;51(2):264–76.
14. Lima KMG, Bedia C, Tauler R. A non-target chemometric strategy applied to UPLC-MS sphingolipid analysis of a cell line exposed to chlorpyrifos pesticide: a feasibility study. Microchem J. 2014;117:255–61.
15. Gorrochategui E, Jaumot J, Tauler R. A protocol for LC-MS metabolomic data processing using chemometric tools. Protocol Exchange. 2015. doi:10.1038/protex.2015.102.
16. Jaumot J, Gargallo R, de Juan A, Tauler R. A graphical user-friendly interface for MCR-ALS: a new tool for multivariate curve resolution in MATLAB. Chemom Intell Lab Syst. 2005;76(1):101–10.
17. Jaumot J, de Juan A, Tauler R. MCR-ALS GUI 2.0: new features and applications. Chemom Intell Lab Syst. 2015;140:1–12.
18. Gorrochategui E, Casas J, Porte C, Lacorte S, Tauler R. Chemometric strategy for untargeted lipidomics: biomarker detection and identification in stressed human placental cells. Anal Chim Acta. 2015;854:20–33.
19. Bedia C, Dalmau N, Jaumot J, Tauler R. Phenotypic malignant changes and untargeted lipidomic analysis of long-term exposed prostate cancer cells to endocrine disruptors. Environ Res. 2015;140:18–31.
20. Farrés M, Piña B, Tauler R. Chemometric evaluation of *Saccharomyces cerevisiae* metabolic profiles using LC–MS. Metabolomics. 2015;11(1):210–24.
21. Grund SS, Hanusch K, Wolf HU. Arsenic and arsenic compounds. Ullmann's encyclopedia of industrial chemistry. Weinheim: Wiley-VCH; 2005.
22. Koek MM, Jellema RH, van der Greef J, Tas AC, Hankemeier T. Quantitative metabolomics based on gas chromatography mass spectrometry: status and perspectives. Metabolomics. 2011;7(3):307–28.
23. Merrill Jr AH, Sullards MC, Allegood JC, Kelly S, Wang E. Sphingolipidomics: high-throughput, structure-specific, and quantitative analysis of sphingolipids by liquid chromatography tandem mass spectrometry. Methods. 2005;36(2):207–24.

24. Tauler R. Calculation of maximum and minimum band boundaries of feasible solutions for species profiles obtained by multivariate curve resolution. J Chemom. 2001;15(8):627–46.
25. de Juan A, Jaumot J, Tauler R. Multivariate curve resolution (MCR). Solving the mixture analysis problem. Anal Methods. 2014;6(14):4964–76.
26. Olson JM, Romano CA. A new chlorophyll from green bacteria. Biochim Biophys Acta. 1962;59(3):726–8.
27. Rocchetta I, Küpper H. Chromium- and copper-induced inhibition of photosynthesis in *Euglena gracilis* analysed on the single-cell level by fluorescence kinetic microscopy. New Phytol. 2009;182(2):405–20.
28. Domonkos I, Kis M, Gombos Z, Ughy B. Carotenoids, versatile components of oxygenic photosynthesis. Prog Lipid Res. 2013;52(4):539–61.